AIP Journal of Applied Physics

Calculation of the threshold current of stripe-geometry double-heterostructure GaAs-Ga1−x Al x A s lasers, including a self-consistent treatment of the current-temperature dependence

T. J. S. Mattos, N. B. Patel, and F. D. Nunes

Citation: Journal of Applied Physics **53**, 149 (1982); doi: 10.1063/1.331590
View online: http://dx.doi.org/10.1063/1.331590
View Table of Contents: http://scitation.aip.org/content/aip/journal/jap/53/1?ver=pdfcov
Published by the AIP Publishing

Articles you may be interested in

Study of intensity pulsations in proton-bombarded stripe-geometry double-heterostructure Al x Ga1−x As lasers
J. Appl. Phys. **50**, 4620 (1979); 10.1063/1.326572

Photoelastic waveguides and their effect on stripe-geometry GaAs/Ga1−x Al x As lasers
J. Appl. Phys. **50**, 4567 (1979); 10.1063/1.326563

Improved light-output linearity in stripe-geometry double-heterostructure (Al,Ga)As lasers
Appl. Phys. Lett. **29**, 372 (1976); 10.1063/1.89091

Saturation of the junction voltage in stripe-geometry (AlGa)As double-heterostructure junction lasers
Appl. Phys. Lett. **28**, 714 (1976); 10.1063/1.88625

Current dependence of spontaneous carrier lifetimes in GaAs–Ga1-x Al x As double-heterostructure lasers
Appl. Phys. Lett. **24**, 486 (1974); 10.1063/1.1655022

SHIMADZU Excellence in Science
Powerful, Multi-functional UV-Vis-NIR and FTIR Spectrophotometers
Providing the utmost in sensitivity, accuracy and resolution for applications in materials characterization and nano research
• Photovoltaics • Ceramics
• Polymers • DNA film structures
• Thin films • Coatings
• Paints • Packaging materials
Click here to learn more

[This article is copyrighted as indicated in the article. Reuse of AIP content is subject to the terms at: http://scitation.aip.org/termsconditions. Downloaded to] IP: 35.8.11.3 On: Tue, 26 Jan 2016 10:59:39

Calculation of the threshold current of stripe-geometry double-heterostructure GaAs-$Ga_{1-x}Al_xA_s$ lasers, including a self-consistent treatment of the current-temperature dependence

T. J. S. Mattos, N. B. Patel, and F. D. Nunes
Instituto de Física "Gleb Wataghin," Universidade Estadual de Campinas, Campinas-13100/SP/Brazil

(Received 12 August 1981; accepted for publication 16 September 1981)

The threshold current density of a stripe-geometry GaAs double-heterostructure laser has been calculated taking into account the influence of the dynamical processes occurring along the junction plane. The calculation includes the effects of a temperature profile, current spreading, carrier diffusion and optical mode losses. The junction current density J, which causes heat generation, is assumed to be temperature dependent. The interdependence between them is taken into account in a self-consistent way. The temperature effect is shown to be particularly important for lasers with narrow stripe widths ($<20\,\mu$m).

PACS numbers: 42.55.Px, 42.60.Da

I. INTRODUCTION

The understanding of laser properties requires the knowledge of the dynamical processes occurring in the active region during laser operation. In particular, the single most important property from a practical point of view, the threshold current density, depends on these processes. The operating characteristics of a laser, including its threshold current density and lifetime, are strongly affected by increasing junction temperature. Temperature changes in the optical cavity induce changes in the band gap of the material and its refractive index. These in turn influence the emission wavelength, current spread, and threshold current density.

In broad area lasers the current flow is one dimensional and the current density in the active region is uniform. In structures such as stripe-geometry lasers, the rapid increase in threshold current density as stripe width decreases suggests the importance of the processes occurring in the direction along the junction plane. The effects of current spreading, carrier out-diffusion, and optical-mode losses greatly influence the threshold current behavior and the emission properties of stripe lasers. These effects have been extensively discussed by Hakki,[1,2] Yonezu,[3] Buus,[4] and Tsang.[5] In these previous works the interdependence between the temperature created in the active region and the injected current was neglected. In our model we analyze the effect of the temperature profile along the junction plane on the above mentioned processes, which influence the threshold current density. The method takes into account the junction current dependence on junction temperature. When a laser is in operation, much of the input power is dissipated as heat, causing an increase in the active region temperature. This induces changes in the junction current density. This dependence is evaluated by an iterative self-consistent calculation. Using the resulting temperature and current profiles, we obtain the carrier distribution in the active region, including carrier out-diffusion. The influence of the spatial variation in temperature and the free carriers on the refractive index of the GaAs active layer is calculated. The optical field distribution of the mode is obtained by treating the problem in both transverse directions. The optical mode distribution thus obtained is used to calculate the optical mode gain and the threshold current density.

The calculations are carried out for spontaneous recombination only. Under this condition, the photon population has negligible effect on carrier concentration. All solutions are assumed to be symmetrical with respect to the center of the stripe.

II. ANALYSIS

A. Self-consistent calculation

The present calculation is carried out for a GaAs-Al_xGa_{1-x}As planar stripe type double-heterostructure (DH) laser,[3,6] operating continuously at room temperature. The laser is shown schematically in Fig. 1. The stripe width is S and its thickness d. The injected current spreads in a layer of thickness t and resistivity ρ. The thickness t can be comprised of one or more layers, in which case the resistivity must be appropriately averaged.[7] The laser length and width are A and B, respectively. Except when specified in the text, we will assume a proton bombardment stripe laser with $S=12\,\mu$m, $t=0.2\,\mu$m, $d=0.2\,\mu$m, $\rho=0.062\,\Omega$ cm, $A=375\,\mu$m and $B=250\,\mu$m.

In order to get the self-consistent current-temperature calculation we have to analyze the potential distribution along the stripe. The potential drop in the x direction under the stripe, i.e., for $|x|\leqslant\frac{1}{2}S$, is negligible because the metallic contact provides uniform current injection. However, for $|x|\geqslant\frac{1}{2}S$ there is a potential drop in x direction due to the finite resistance of the spreading layer in this direction. The junction voltage beyond the stripe edges is given by the solution of the equation

$$\frac{d^2V(x)}{dx^2}=\rho\frac{J_0}{t}\exp[\beta V(x)], \tag{1}$$

where $\beta=q/nkT$ (T is the temperature, k is the Boltzmann constant, q is electronic charge, and J_0 is the saturation current density, which is temperature dependent). This equa-

 0021-8979/82/010149-07$02.40 © 1982 American Institute of Physics

[This article is copyrighted as indicated in the article. Reuse of AIP content is subject to the terms at: http://scitation.aip.org/termsconditions. Downloaded to] IP: 35.8.11.3 On: Tue, 26 Jan 2016 10:59:39

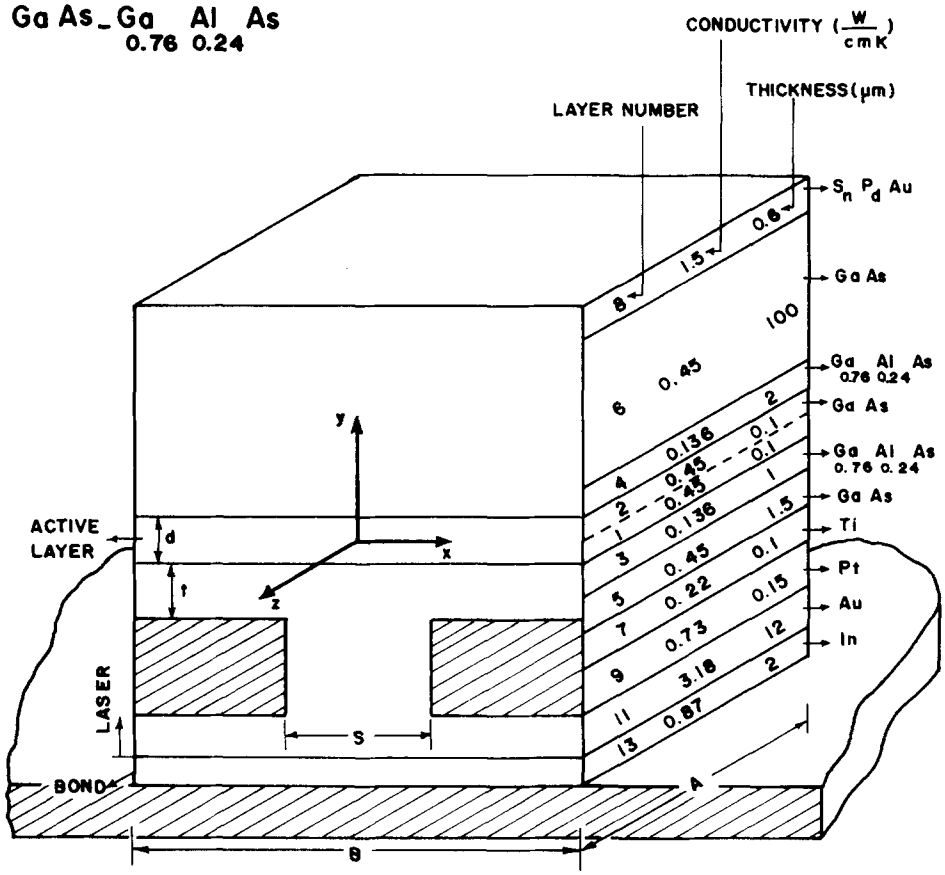

FIG. 1. Illustration of a planar stripe laser used in the calculation (not in scale).

tion is equivalent to Eq. (4) in Ref. 2.

The solution of Eq. (1) is

$$V(x) = V_0, |x| \leqslant S/2$$

$$V(x) = \beta^{-1}\{\ln(2m^2) + \ln \sec^2[mK^{1/2}(x - B/2)]\}, \quad (2)$$

$$|x| \geqslant S/2,$$

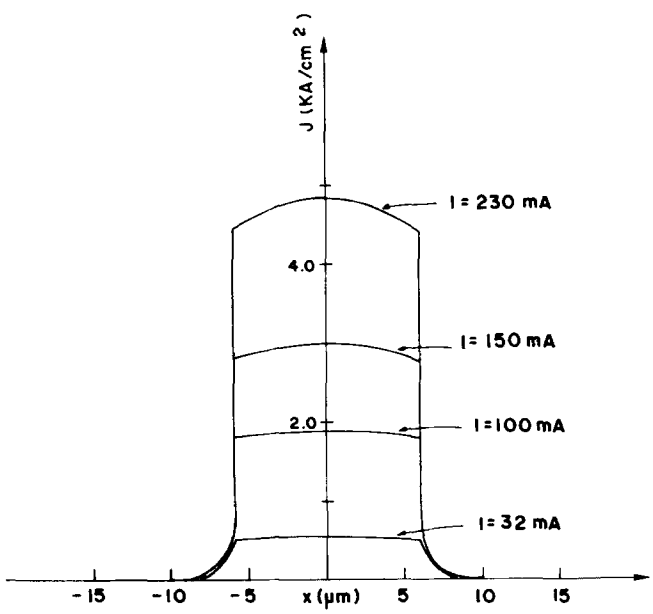

FIG. 2. Current density profiles, calculated for different injection levels.

where m is an integration constant and $K = J_0\beta\rho/t$. Both m and K are temperature-dependent constants.

The current density across the junction is given by

$$J(x) = J_0 \exp[\beta \times V(x)]. \quad (3)$$

If there is a temperature gradient along the x direction, $J(x)$ at each point x of the active layer will depend on temperature, explicitly through the temperature dependence of J_0 and β, and implicitly through V [Eq. (2)].

The temperature profile $T(x)$ along the junction plane is calculated as proposed by Joyce and Dixon.[8] In their model, heat is generated uniformly and steadily in a planar stripe source which is embedded in a rectangular layered structure. The heat generation rate Q per unit area is the product of the device current density times the applied voltage, less the optical output. Up to threshold the external quantum efficiency is less than 5%, and the optical output power can be ignored, so

$$Q(x) = V(x) \times J(x). \quad (4)$$

Assuming $Q(x)$ as step function in the x direction, an initial temperature distribution $T(x)$ is calculated. This temperature profile induces changes in $V(x)$ and $J(x)$ [Eqs. (2) and (3)]. As a consequence $Q(x)$ changes also. The new $Q(x)$ can be well approximated by a step function, and the iterative process is repeated until changes in $Q(x)$ are less than 0.001%. It is worth noting that the process is convergent only up to a certain value of external voltage V_0 applied to the diode, beyond which the mutually reinforcing increase in $J(x)$ and $T(x)$ results in a nonconverging runaway process. In

[This article is copyrighted as indicated in the article. Reuse of AIP content is subject to the terms at: http://scitation.aip.org/termsconditions. Downloaded to] IP: 35.8.11.3 On: Tue, 26 Jan 2016 10:59:39

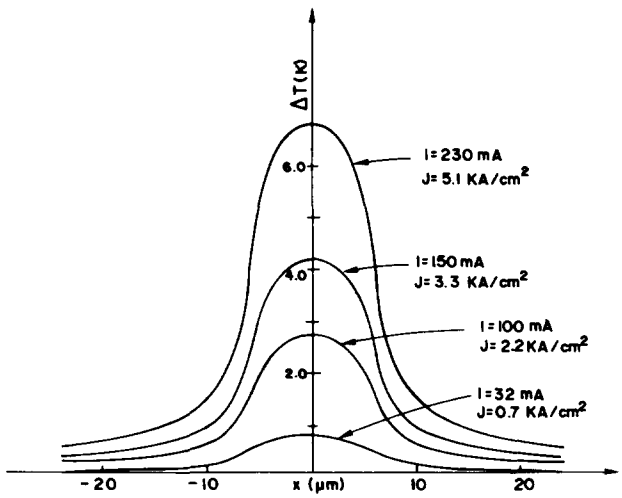

FIG. 3. Temperature distribution profiles corresponding to the current density profiles shown in Fig. 2.

practice, the series resistance of the external circuit feeding current to the diode will limit this runaway process.

The resulting current density profiles are shown in Fig. 2 for different injection currents. We observed that the current density is strongly confined within the stripe region. This confinement is independent of the external applied voltage V_0 and is mainly influenced by the resistivity (ρ) of the spreading layer.

The temperature distributions corresponding to the shown current density profiles are illustrated in Fig. 3. We observed that even though the current density is confined to the stripe region, the temperature is not. About 40% of the temperature drop occurs within the active region. The temperature profile is not much affected by changing the resistivity ρ and the thickness t but is affected by changing the stripe width S and the carrier diffusion length L (through the dependence of J with L).

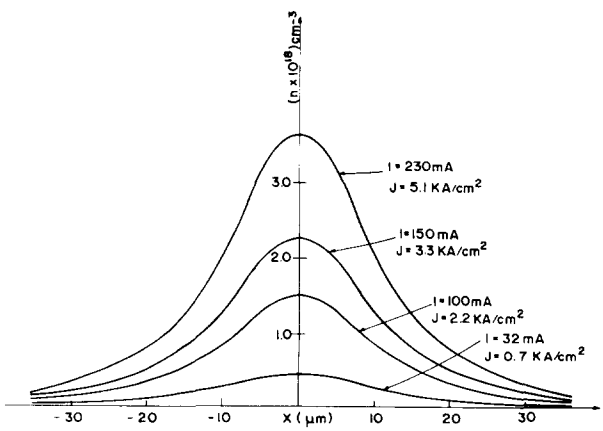

FIG. 4. Calculated carrier density profiles.

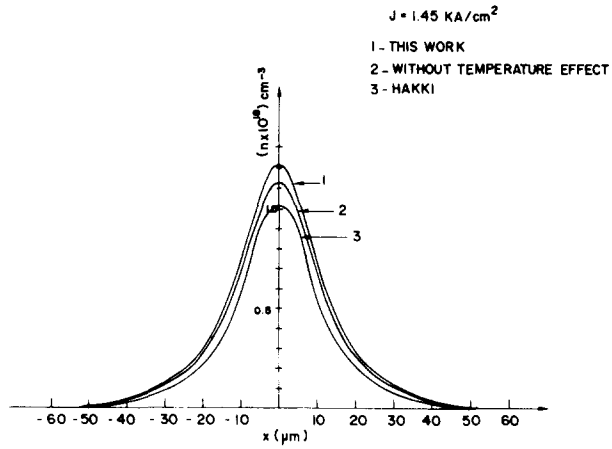

FIG. 5. Calculated density profiles due to different processes.

The carrier concentration profile $n(x)$ is numerically calculated from the final $J(x)$ profile. Because of the long minority carrier diffusion length, a significant amount of carrier diffusion occurs in both x and y directions. The carrier diffusion in the y direction can be assumed as instantaneous,[1] since the thickness of the active region is extremely small in comparison with the diffusion length. The lateral carrier diffusion results in a carrier concentration that can be quite different from the injected current profile.

The carrier concentration profile due to lateral diffusion may be found from the continuity equation

$$\frac{d^2n}{dx^2} = \frac{n - n'(x)}{L^2}. \tag{5}$$

In this equation $n'(x) = J(x)/\tau qd$ is the carrier concentration generated by the injected current density $J(x)$, and τ is the carrier lifetime.

If L can be assumed independent of the carrier density[1] (maximum carrier density at threshold is $\sim 1.5\times 10^{18}$ cm^{-3}), Eq. (5) is linear and can be numerically solved, imposing the condition of conserving the total number of electrons. The factorization method[9] employed in the calculations allowed us to calculate the $n(x)$ profile shown in Fig. 4, for a p type GaAs active layer ($L_n = 10\,\mu m$). It is important to note that the half-widths do not change appreciably with injection current. This is in agreement with the experimental results obtained by Paoli,[10] that the width of the spontaneous emission is essentially independent of the current level. The carrier density profile for a proton bombardment stripe-geometry DH laser was also discussed by Hakki,[1] by solving Eq. (5) for two separated regions $|x| \leqslant S/2$ and $|x| \geqslant S/2$, and requiring the continuity of carrier concentration and current density at $x = S/2$.

In order to compare different methods, Fig. 5 shows the carrier density profiles resulting from this work with (curve 1) and without (curve 2) the current-temperature dependence. This result is also compared with Hakki's results for the same initial injection current. The difference between curves 2 and 3 is essentially due to the calculation methods. The difference between curves 1 and 2 are due to the reinforcing current-temperature-dependent process.

[This article is copyrighted as indicated in the article. Reuse of AIP content is subject to the terms at: http://scitation.aip.org/termsconditions. Downloaded to] IP: 35.8.11.3 On: Tue, 26 Jan 2016 10:59:39

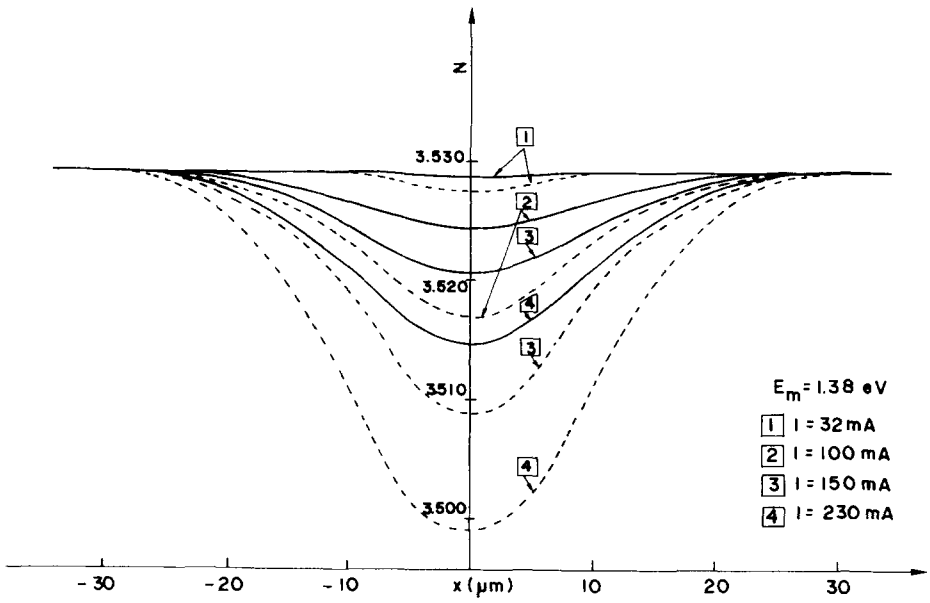

FIG. 6. Refractive index profiles due to the presence of free carriers (dashed line) and as calculated by Eq. (6) (solid line).

B. Refractive index and gain profiles: threshold condition

Current spreading, lateral carrier diffusion, and temperature profiles have significant effects on the dielectric constant of the GaAs-active layer, which in turn, induces changes in the optical waveguide. In this section we calculate the refractive index and local gain profiles that arise along the junction plane, taking into account the effects described above. We find that both refractive index and local gain profiles can be well described by an analytical function, and therefore the optical mode distribution can be evaluated. The threshold condition is attained when the gain acquired by the mode equals the total losses in the cavity.

The effect of injected free carriers on the refractive index N of the GaAs active layer was extensively discussed by Mendoza-Alvarez *et al.*[11] From their data and the carrier density profiles calculated in this work, we were able to get the refractive index profiles shown in Fig. 6. The dashed lines represent the refractive index profile due to the presence of free carriers only (N_{fc}). In order to combine the contributions from the free carriers and temperature into an effective refractive index, we assumed, as suggested in Ref. 10, that

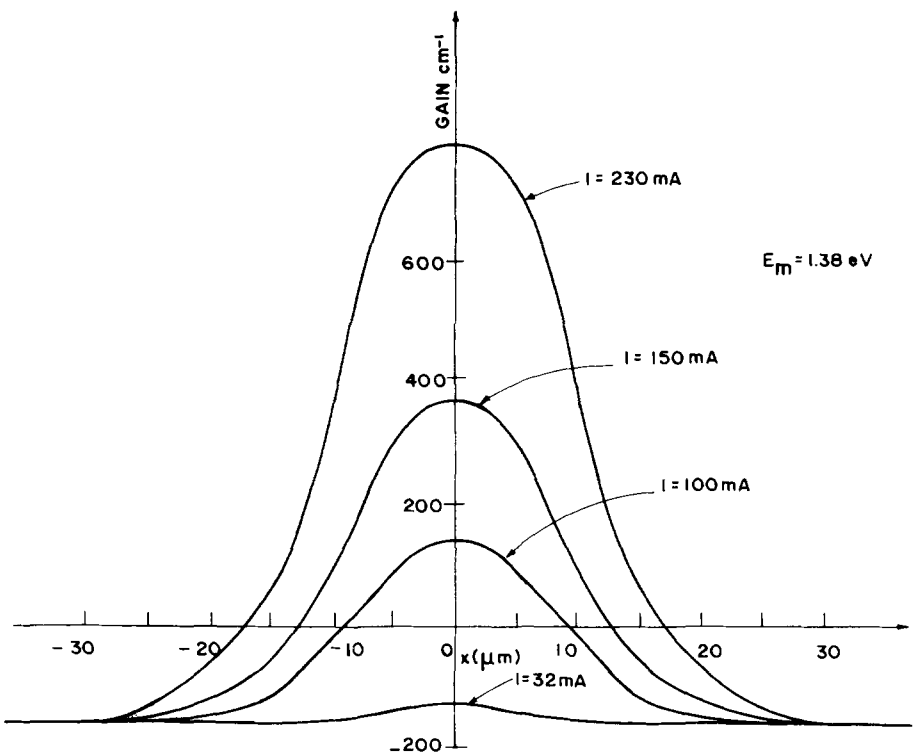

FIG. 7. Calculated gain profiles.

[This article is copyrighted as indicated in the article. Reuse of AIP content is subject to the terms at: http://scitation.aip.org/termsconditions. Downloaded to] IP: 35.8.11.3 On: Tue, 26 Jan 2016 10:59:39

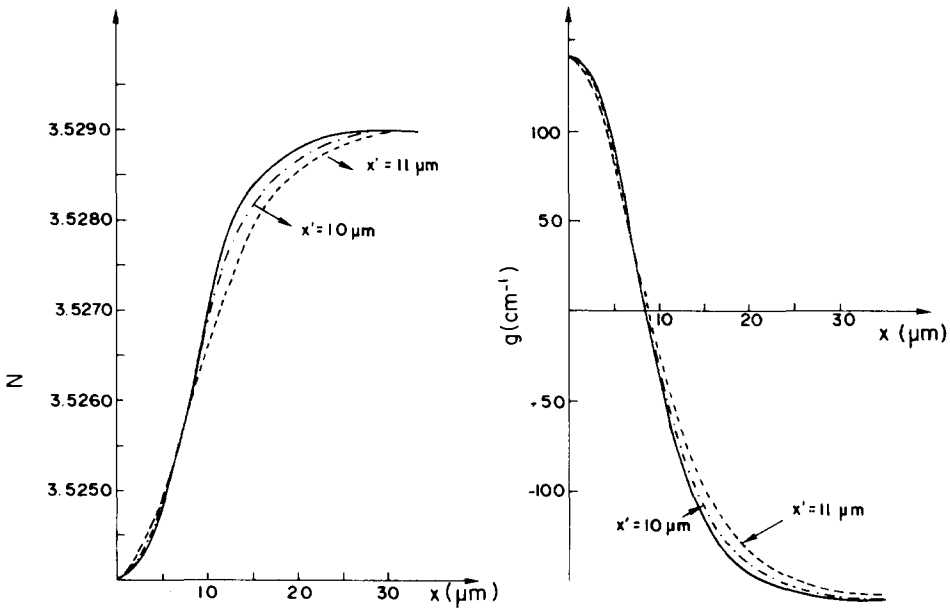

FIG. 8. Example of the fitting to the numerical data by the functions given by Eqs. (7) and (8).

$$(\Delta N)_{\text{eff}} = \Gamma(\Delta N)_{\text{fc}} + \frac{\partial N}{\partial t}\Delta T, \tag{6}$$

where $\partial N/\partial T = 5\times 10^{-4}$ (Ref. 12) and Γ is the confinement factor for the DH waveguide.

The resulting net refractive index profiles are shown as full lines in Fig. 6. Figure 7 shows the corresponding gain profiles due to the presence of free carriers. From Figs. 6 and 7 we observe that, for proton bombardment stripe laser, the temperature effect is not enough to compensate the defocusing effect due to the free carrier density, contrary to that suggested by Paoli.[10] The light confinement along the junction plane is due to a gain profile.

The numerically-calculated curves for the refractive index N and the local gain g can be represented by the smoothly varying symmetric functions

$$N(x) = \{N_0^2 - 2\delta N_0[1 - \text{sech}^2(x/x')]\}^{1/2}, \tag{7}$$

$$g(x) = g_0 - \Delta\,[1 - \text{sech}^2(x/x')], \tag{8}$$

where δ is the maximum value of the refractive index hump; Δ is the maximum value of the gain hump; N_0 and g_0 are the values of N and g at $x = 0$; x', a measure of the half-width of the hump, is the same for both the functions.

Equation 7 for the refractive index is the same as used in Ref. 13 to explain the resonant mode behavior of the GaAs lasers, except that, in this reference, the effect of the gain profile was included in the real refractive index to produce a positive hump δ. In our case, gain is treated separately, and the refractive index hump is negative, so δ is negative.

The $n(x)$, $g(x)$, $N(x)$ profiles have almost identical (to within 5 or 10 percent) half-widths at half intensity. The value of x' equal to the half-width gives the best fit of both the functions (7) and (8) to the numerically calculated values. Figure 8 illustrates the fitting to the numerical data. It is important to note that the value of x' is not so critical, in the sense that a variation of 25% in its value leads to a variation of about 4% in the threshold current density J_{th}.

The dielectric constant ϵ along x direction, obtained from Eqs. (7) and (8), is

$$\epsilon(x) = \epsilon_\infty + \Delta\epsilon\ \text{sech}^2(x/x'), \tag{9}$$

where $\Delta\epsilon = 2N_\infty(\delta - i\Delta')$. (10)

Here ϵ_∞ and N_∞ are the undisturbed values of ϵ and N for large x and $\Delta' = (\lambda/4\pi)\Delta$.

The resulting waveguide modes may be obtained by treating the waveguide as a two-dimensional one. The electric field distribution in the y direction is given by the usual optical field distribution $E_0(y)$ in a three-layer structure with the center layer as waveguide. The portion of the propagating mode within the active layer is represented by the confinement factor Γ. In the x direction, the resulting waveguide modes may be obtained from the wave equation

$$\frac{d^2E}{dx^2} + k_0^2[\epsilon_\infty + \Delta\epsilon\ \text{sech}^2(x/x')]E = \gamma^2 E. \tag{11}$$

Here γ is the propagation constant and $k_0 = 2\pi/\lambda$. The solution for the zero-order mode is[14]

$$E_0(x) = \phi\ \cosh^{-b_0}(x/x'), \tag{12}$$

with

$$b_0 = (k_0^2 x'^2 \Delta\epsilon + 1/4)^{1/2} - 1/2. \tag{13}$$

The net gain for mode $E_0(x, y)$ is given by

$$G = \Gamma\frac{\int_{-\infty}^{\infty} g(x)|E_0(x)|^2 dx}{\int_{-\infty}^{\infty}|E_0(x)|^2 dx}, \tag{14}$$

where Γ reflects the fact that the optical distribution along the junction plane is indeed influenced by that in the perpendicular direction.

The threshold condition is attained at the injection current for which the gain equals the total losses in the cavity. For a DH laser the main loss mechanisms are diffraction losses ($\propto_{\text{dif}}$), free-carrier losses ($\propto_{\text{fc}}$), and mirror losses. Remembering that diffraction losses are included in the integration of Eq. (14), the threshold condition is given by

[This article is copyrighted as indicated in the article. Reuse of AIP content is subject to the terms at: http://scitation.aip.org/termsconditions. Downloaded to] IP: 35.8.11.3 On: Tue, 26 Jan 2016 10:59:39

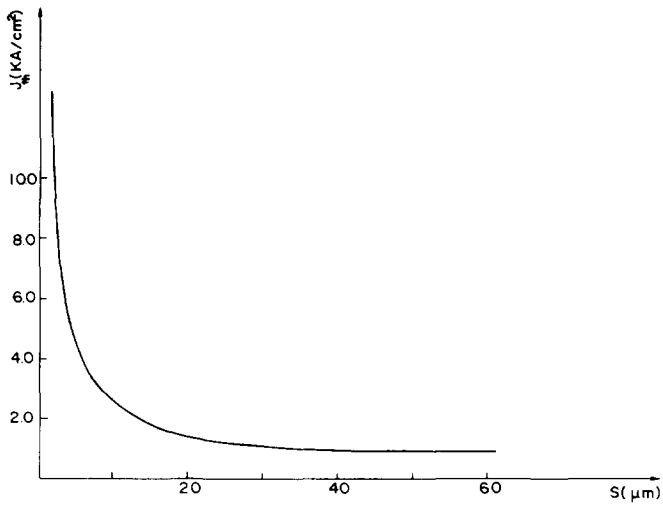

FIG. 9. Threshold current density variation as function of stripe width for a proton bombardment laser.

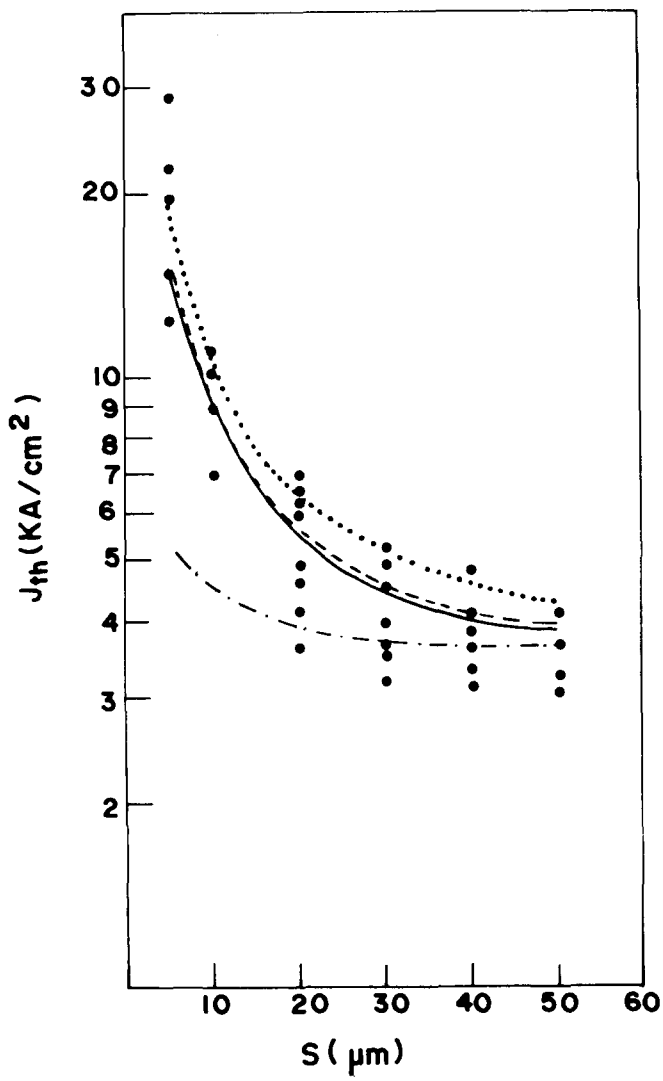

FIG. 10. Variation of J_{th} with S for the planar stripe laser described in Ref. 3. The solid dots are experimental points[3]; the solid curve is calculated in this work for $L_n = 6.0\,\mu$m; the dotted curve is calculated in this work neglecting temperature influence. These curves are compared with the results of Ref. 3 for current spreading only (dot-dash curve), and the results of Ref. 5 for $L_n = 8.0\,\mu$m (dashed curve).

$$G = \alpha_{fc} + 1/A \ln(1/R). \tag{15}$$

III. RESULTS AND DISCUSSION

In this section the theory presented above will be used to calculate J_{th} and ΔT and will be compared with some experimental results obtained for proton bombardment and planar stripe lasers.

Figure 9 shows the threshold current density variation as stripe width is decreased for the laser described in Sec. II. For this laser $d = 0.2\,\mu$m, which gives $\Gamma = 0.5$,[15] and $\tau = 5.9$ nsec.

The $J_{th}xS$ variation for a planar stripe laser is compared with the experimental data obtained by Yonezu *et al.*[3] The lasers are 300-μm long and have a 0.7-μm active region thickness. The spreading layer has $t = 2.0\,\mu$m and $\rho = 0.2$ Ω cm. For the growth condition described (2.5 mg Ge/gr de Ga) $L_n = 6\,\mu$m,[16–18] $\tau \simeq 3.5$ nsec, and $\Gamma = 0.98$.[15] The metallic contact is gold, and in the calculation we assume an ideal heat sink. In Fig. 10 the dots are experimental points. The solid line is the result of this work. It is worth noting that our result is almost coincident with Tsang's[5] result for $L_n = 8.0$ μm (dashed line), but the value of $L_n = 6.0\,\mu$m is more realistic. Our results for $L_n = 8.0\,\mu$m is almost coincident with the curve obtained when the temperature influence is neglected and $L_n = 6.0\,\mu$m (dotted line). The dash-dot line includes the effect of current spreading only, as calculated in Ref. 3. The increase in J_{th} with increasing L_n is due to an increase in the diffraction loss due to the carrier diffusion to the lossy region. In order to avoid an overestimation of the threshold current density, we have to take into account the temperature effects, especially for a stripe laser width less than $20\,\mu$m. The overestimation in the values of J_{th} for laser width up to $60\,\mu$m is shown in Fig. 11.

Figure 12 shows the maximum temperature variation at threshold, calculated for the proton bombardment laser and planar stripe laser described above. The temperature in-

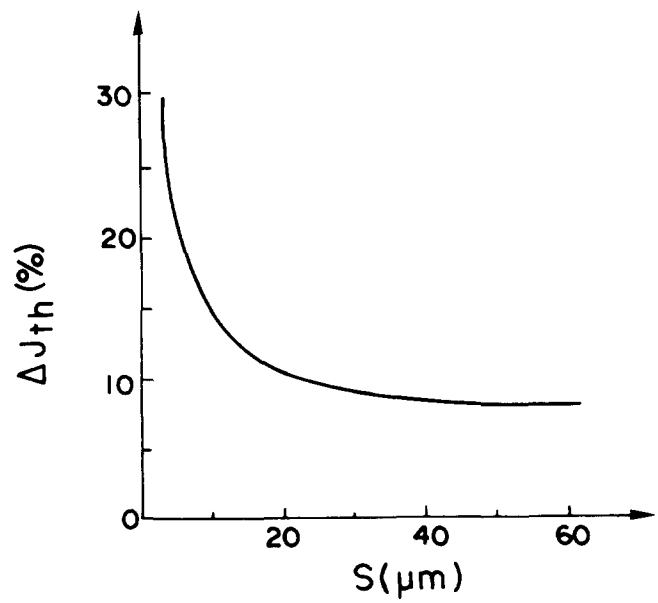

FIG. 11. Overestimation in J_{th} neglecting temperature effects.

[This article is copyrighted as indicated in the article. Reuse of AIP content is subject to the terms at: http://scitation.aip.org/termsconditions. Downloaded to] IP: 35.8.11.3 On: Tue, 26 Jan 2016 10:59:39

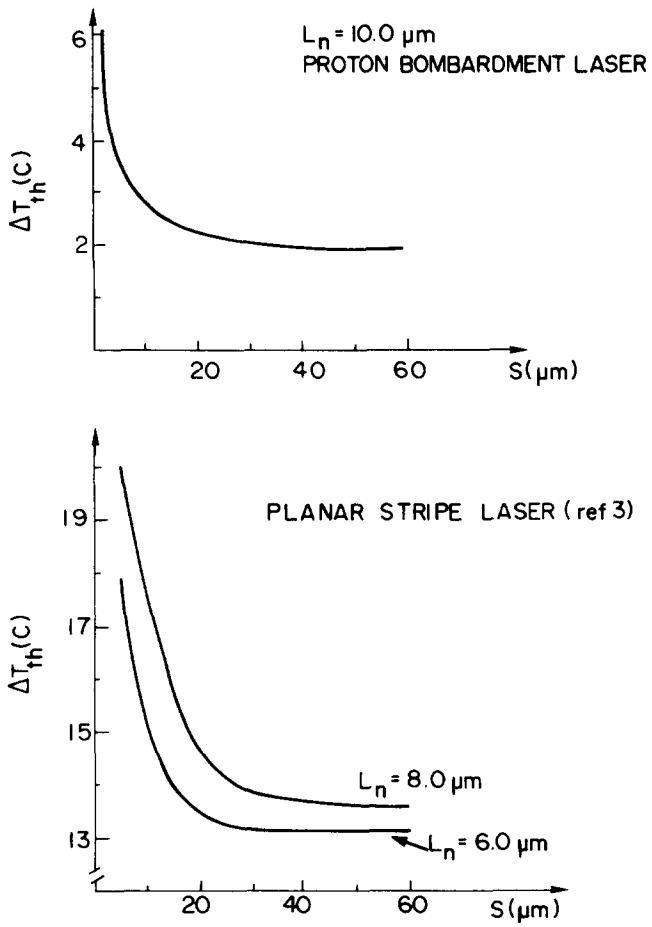

FIG. 12. Maximum temperature variation at threshold for the proton bombardment and planar stripe lasers described.

crease as stripe width decreases is, as expected, due to the increase in the threshold current density. This calculation assumes that the laser is on an ideal heat sink. In practice, the influence of the heat sink has to be taken into account in terms of the heat-sink thermal resistance, as already discussed by Joyce and Dixon.[8] In order to compare the calculated ΔT with the corresponding experimental value, the junction temperature rise was experimentally measured using Paoli's null method.[19] For a 7-μm stripe width and 380-μm long proton bombardment laser, on a copper heat sink, the temperature rise measured was 4.6 °C at 3.5 kA/cm^2. This value is in excellent agreement with the calculated value of 4.4 °C at the same current density. For the 20 μm stripe-width planar-stripe laser described, on copper heat sink the calculated value of temperature rise is 17.7 °C at 5 kA/cm^2. This value is comparable with the measured value of 20 °C measured by Yonezu *et al.*[3]

For all lasers (proton bombardment and planar stripe lasers) investigated, the temperature effect was not enough to compensate the defocusing effect of the refractive index, due to the presence of free carriers. The mode confinement along the junction plane for these lasers was due to the gain profile. Only for a planar stripe laser with a stripe width less than 5 μm and a diffusion length of 8 μm, did we obtain a positive contribution to the refractive index of the active region. In this case, the temperature rise must be about 20 °C in order to get a 1% variation of N and result in a refractive index mode guiding.[10,13]

ACKNOWLEDGMENTS

We are grateful to J. C. Mendoza-Alvarez for useful discussion and to J. C. V. Mattos for his continuous encouragement.

[1]B. W. Hakki, J. Appl. Phys. **44**, 5021 (1973).
[2]B. W. Hakki, J. Appl. Phys. **46**, 292 (1975).
[3]H. Yonezu, I. Sakuma, K. Kobayashi, T. Kamejima, M. Ueno, and Y. Nannichi, Jpn. J. Appl. Phys. **12**, 1585 (1973).
[4]J. Buus, Opt. Quantum Electron. **10**, 459 (1978).
[5]W. T. Tsang, J. Appl. Phys. **49**, 1031 (1978).
[6]L. A. D'Asaro, J. Lumin. **7**, 310 (1973).
[7]W. B. Joyce and S. H. Wemple, J. Appl. Phys. **41**, 3818 (1970).
[8]W. B. Joyce and R. W. Dixon, J. Appl. Phys. **46**, 855 (1975).
[9]D. R. Hartree, *Numerical Analysis*, 2a ed. (Oxford University, London, 1958), p. 161.
[10]T. L. Paoli, IEEE J. Quantum Electron. **13**, 662 (1977).
[11]J. G. Mendoza-Alvarez, F. D. Nunes, and N. B. Patel, J. Appl. Phys. **51**, 4365 (1980).
[12]F. R. Nash, J. Appl. Phys. **44**, 4696 (1973).
[13]F. D. Nunes, N. B. Patel, J. G. Mendoza-Alvarez, and J. E. Ripper, J. Appl. Phys. **50**, 3852 (1979).
[14]D. F. Nelson and J. McKenna, J. Appl. Phys. **38**, 4057 (1967).
[15]H. C. Casey and M. B. Panish, *Heterostructure lasers* (Academic, New York, 1978) A p. 53.
[16]F. E. Rosztoczy and K. B. Wolfstirn, J. Appl. Phys. **42**, 426 (1971).
[17]H. C. Casey, B. I. Miller, and E. Pinkas, J. Appl. Phys. **44**, 1281 (1973).
[18]H. Schade, H. Nelson, and H. Kressel, Appl. Phys. Lett. **18**, 121 (1971).
[19]T. Paoli, IEEE J. Quantum Electron. **11**, 498 (1975).

[This article is copyrighted as indicated in the article. Reuse of AIP content is subject to the terms at: http://scitation.aip.org/termsconditions. Downloaded to] IP: 35.8.11.3 On: Tue, 26 Jan 2016 10:59:39